6th Intercontinental Geoinformation Days

igd.mersin.edu.tr

Using EO1 hyperspectral images for rock units mapping

Parisa Safarbeyranvand [1], Parviz Zeaiean Firouzabadi [*2], Ali Hosingholizade[3], Reza Bastami[4]

[1] *Kharazmi University, Geography, Remote sensing and GIS, Tehran, Iran*
[2] *Tehran University, Geography, Remote sensing and GIS, Tehran, Iran*
[3] *Islamic Azad University Science and Research Branch, Tehran, Iran*

Keywords
Hyperspectral Images
Rock Plot
Pure Members
SAM
SVM

Abstract

The issue of mapping geological units during an evolving process has now reached a point where the detection and classification of geological units is carried out with the aid of hyperspectral sensing. In this study, using hyperspectral the image of the Hyperion sensor, related to the Khorramabad area in Lorestan province, and using Spectral Angle Mapper (SAM) and SVM (Support Vectors Machine) algorithms for detecting and separating geological units after performing the necessary preprocesses, the MNF conversion and PPI algorithm were used to reduce data and extract pure pixels on the image, respectively. From the overlapping of pure pixels with geological units and ground data, the average range for each member was extracted. Field surveys performed at the points provided by the Spectral Angle Mapter (SAM) confirm the superiority of the SVM method in separating geological units. Finally, by verifying the accuracy of the algorithms by calculating the error matrix, the accuracy of the classification of each method are (68.83) and (81.70) is for SVM and SAM respectively, it was found that at the end of the SVM algorithm with a total accuracy of 81.70 was introduced as the best classification algorithm.

1. Introduction

Using remote sensing technology and using satellite data reduced the costs and increased accuracy and speed of data collecting (Alvipanah, 2013). The use of satellite technology in the last decades as one of the most important means of information acquisition attracted the attention of many experts and specialists of various sciences, including geology, mining, environment, meteorology, agriculture and etc. From years of 1980, by introducing of Hyper-spectroscopic sensors, a major step has been taken in the area of remote sensing technology (Hasani Moghaddam, 2019). Hyper-spectral sensors, in comparison with multi-spectral sensors, produce much more accurate spectral data and therefore allow for more accurate identification of ground targets (Campsvalls et al., 2014). As the Hyper-spectral sensors are used of bands extremely large spectra produce a large amount of spectral data, so it is also necessary to use methods that are capable of processing and extracting valuable information from this high dimension data. The relationships of geological and remote sensing are nearly thirty years old (Waske et al., 2009). In the most hyper spectral sensors, reflection measurements of surface phenomena with a spectral width of 0.01 μm and spectral ranges of 0.4 to 2.5 μm are acquired, so this property makes it possible for geological unit's investigations.

The existing maps of the geological units are prepared by traditionally ways; in this research, used of remotely sensed hyperspectral images to produce more accurate maps of geological units. The data obtained from the measurements in terms of providing a wide coverage of the area and providing quantitative parameters can be a suitable source for updating geological maps (Rajendran et al., 2007). Images from remote sensing technology provide efficient data that requires processing on the image to extract information from them.

Among different methods of remote sensing, the classification techniques have a special role in analyzing, separating and detecting various geological units.

Image classification is one of the main process components of the information extracting from an object that are obtained by examining the relationship between spectral effects and classes (Oommen et al., 2008).

Ramakrishnan and Bharati (2015), review the potential of Hyperspectral Remote Sensing (HRS) technique in various geological applications ranging from lithological mapping to exploration of economic minerals of lesser crustal abundance. This work updates

* **Corresponding Author**
(pbeyranvandgis@gmail.com) ORCID ID 0000 – 0002 – 7860 – 2621
*(p.zeaiean@gmail.com) ORCID ID 0000-0001-8407-5605
(a.hosingholizade@ut.ac.ir) ORCID ID 0000 – 0001 – 5286 – 1361
(Bastami870@gmail.com) ORCID ID 0000 – 0000 – 0000 – 0000

Cite this study
Safarbeyranvand, P., Firouzabadi, P. Z., Hosingholizade, A., & Bastami, R. (2023). Using EO1 hyperspectral images for rock units mapping. Intercontinental Geoinformation Days (IGD), 6, 191-194, Baku, Azerbaijan

understanding on the subject starting from spectroscopy of minerals to its application in exploring mineral deposits and hydro-carbon reservoirs through different procedures such as atmospheric correction, noise reduction, retrieval of pure spectral endmembers and unmixing.

In this research, we specifically seek to compare the classification of geological units using SVM and SAM methods and compare them.

2. Method

2.1. Study area

The study area is located in the west of Iran, Lorestan province, Khorramabad city. Khorramabad is geographically located at 33 degrees, 29 minutes north latitude and 48 degrees, 21 minutes east.

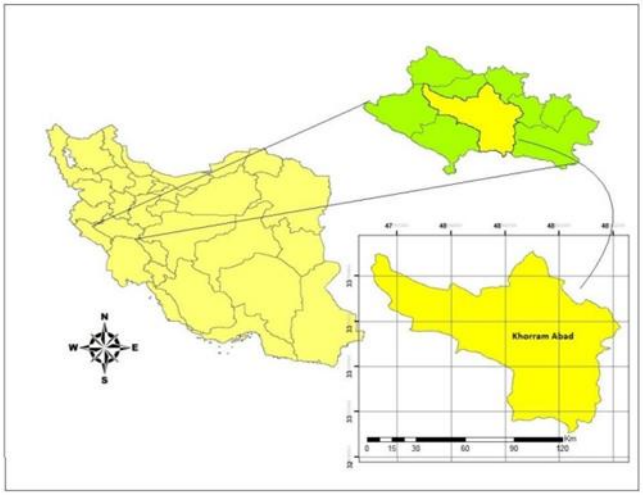

Figure1. Iran and case study

2.2. Satellite Image of EO-1 Hyperion Sensor

The image used in this study was captured in September 5, 2010, with a route number 166 and a row number 37. Its dimensions are 7.65 km wide and 185 km long. The centre of this area is the coordinates of 31° 37'00.09 "north and 47 ° 53'19.11" east.

2.3. Band Selection

Among the 242 spectral bands of the Hyperion sensor used in this research, 196 bands are calibrated and unique, and 155 bands were entered into the processing stage by removing the bands that absorb water or have a lot of noise. Table 1 shows the range of acceptable electromagnetic wavelengths for entering the processing stage.

Table 1. Acceptable bands which enter processing

Acceptable bands	Spectral range
8-57	VNIR range
79 83-119 133-164 183-184 188-1220	SWIR range

2.4. Minimum noise fraction

Transform (MNF) reduces data dimensionality and noise when using hyperspectral data. The MNF transform is considered as a noise reduction transform. It is a linear transformation that is used to determine the original dimensions and volume of the image, separate noise from other information and reduce the degree of processing in the next step. In this conversion, the image is first converted to noise and noise-free, then the noise-free part is considered as the main part and the noise is removed.

2.5. Pixel Purity Index (PPI)

PPI algorithm is used in hyperspectral images to find pure pixels (final pixels). For this purpose, the ten output bands obtained from the MNF transformation, which are noise-free, are given as input to the PPI algorithm. The output of this algorithm is an image that specifies pure pixels.

2.6. Endmember spectrum extraction through pure pixel identification

Many classification algorithms in hyperspectral images need to enter the spectral characteristics of the members (any class or complex that is classified or revealed in the hyperspectral image is called a member) to start processing.

Pure members were extracted from areas where the type of geological unit was identified. With 4 stages of surveying and field surveying and recording the coordinates of geological units using a high-precision GPS device and using the sampled points that corresponded to the pure pixels extracted from the PPI algorithm, the average reference spectrum of the units was extracted from the image itself and this reference spectrum was used as an input for the classification algorithm (Figure 2).

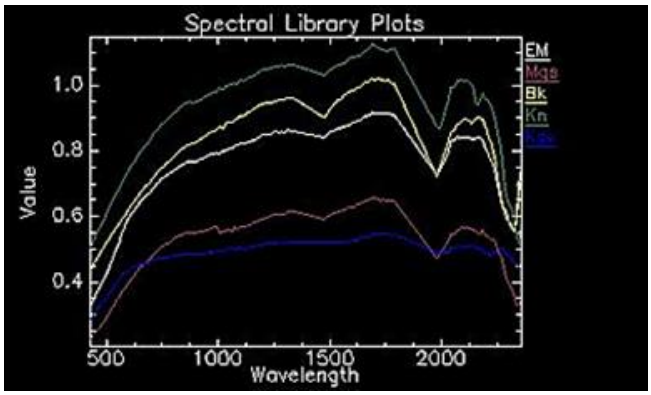

Figure 2. The spectra extraction from the geological unit's image

2.7. Spectral Angle Mapper (SAM)

Spectral Angle Surveyor as a Guided Classification Method, an Effective Method for Spectrum Comparison Images are relative to the standard range or reference spectrum. The algorithm of this method calculates the similarity between the two spectra by the spectral angle

between the two. In fact, by transforming the spectra into a vector in space, the size of the number of bands, the angle between the two vectors is calculated. In this method, for calculating the angle, the direction of the vectors is important and not their length, and therefore, the pixel brightness does not affect their classification. The angle between 0 and 1 if below, the more accurate it will be. If the angle is one, the entire image is identified as the

For example, to compare a pixel, the desired pixel spectrum with the same pixel spectrum is plotted between the reference spectra on two bands in a coordinate axis. The resulting points are then drawn to the origin and the angle between the two resulting lines is known as the pixel identification angle.

2.8. Support Vector Machine (SVM)

Support vector machine is a useful technique for data classification (Abbasi et al., 2015). A classification task usually involves separating data into training and testing sets. Each instance in the training set includes one "target value" (i.e., the class labels) and several "attributes". The goal of SVM is to produce a model which predicts the target values of the test data given only the test data attributes (Wei Hsu et al., 2003).

3. Results

After compilation of classified pictures, to assess the accuracy of each method, the GPS points taken by ground observations were used as ground maps to determine the accuracy of the error matrix, the accuracy of classification in each method, and ultimately the best way to estimate the geological map of the units introduced. The results of a accuracy assessment are usually presented as an error matrix, whereby a variety of parameters and values representing accuracy or some kind of error in the results are extracted from this matrix. This matrix is the result of a comparison of the pixels to pixels, the pixels defined with the corresponding pixels in the classification results. In the error matrix, land data in the columns and data related to the classification results are given in the rows of this matrix. The numbers on the matrix's main diameter indicate the number of pixels whose labels match the two sets of data or, in the other hand, the number of pixels that are correctly categorized over this diameter. Non-diagonal elements are the set of errors.

4. Discussion

The evaluation of the results of this research shows that the mapping of geological units mapped using SAM and SVM algorithms is highly consistent with the maps of the Geological Organization.

The SVM algorithm with overall accuracy of 81.70% and kappa coefficient of 0.72% was more accurate than the SAM algorithm with total accuracy of 68.63% and coefficient of 0.44%. Also, the results show that the SVM algorithm is an effective method for classifying the area based on the existing geological units in geological mapping research, taking into account the regional conditions. Due to the high capability of images in distinguishing phenomena, it has been shown that identification and separation of geological units using these images is easier and more accurate than other methods such as using multi-dimensional images.

According to the results of calculating the area of different formations in the study area, Keshkan formation has the largest area calculated by SVM class and Gachsaran formation has the largest area calculated by SAM classification method.

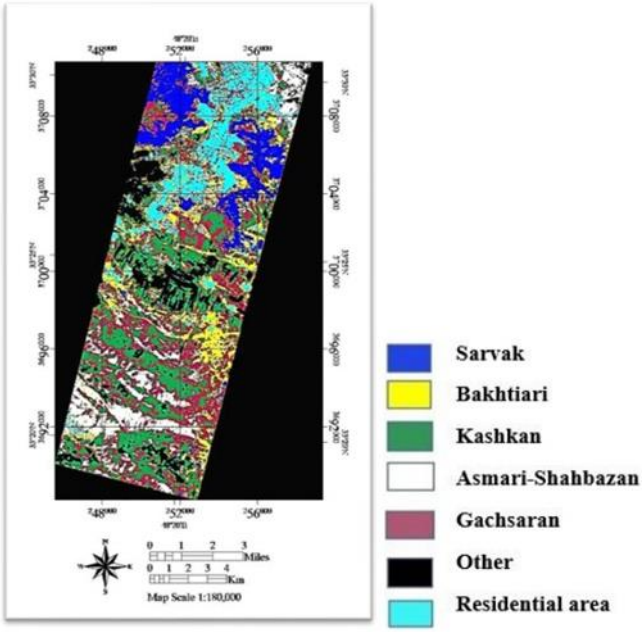

Figure 3. Classification result with SAM algorithm

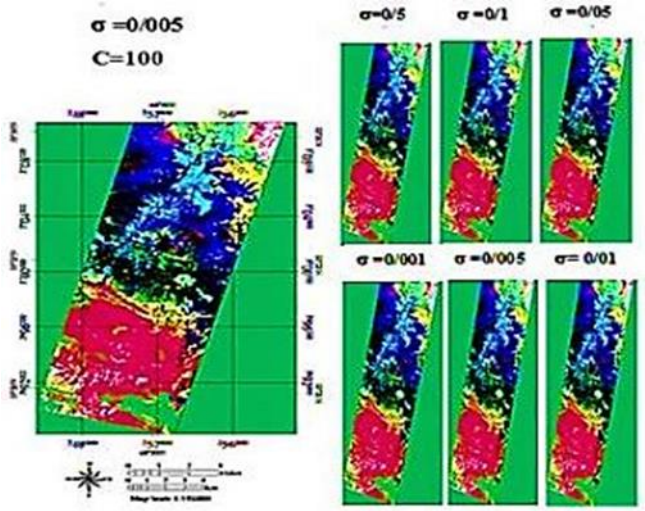

c

σ	C	Maximum precision(%)
≥0/001	100-200	62/57
0/005	100-200	81/70
0/01	100-200	59/96
0/05	100-200	63/01
0/1	100	55/78
	200	61/54
	200-2000	52/85
≥0/5	100-200	76/92

b

Figure 4. Classification result with SVM algorithm

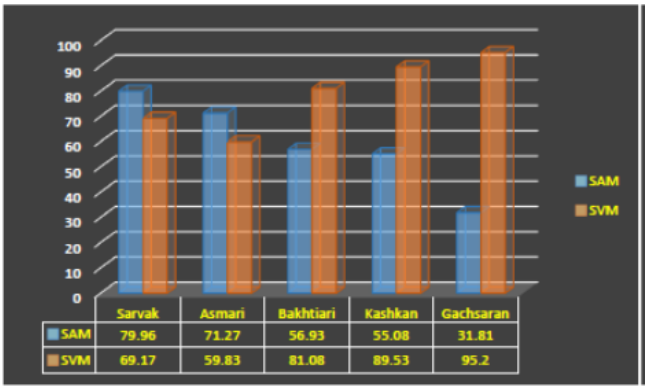

Figure 5. Comparison of the accuracy of the different formation's detection by classification algorithms

5. Conclusion

Over the past years, geological mapping and extensive studies have reached a point where instead of doing field work and spending a lot of time and money, it is possible to study the area in a short time and with high accuracy using remote sensing images.

In this research, SAM and SVM algorithms were used to identify geological units. One of the most important factors in target detection that affects the final evaluation of algorithms is the selection of the threshold value, which was determined by trial and error in this study.

For better identification of geological units, MNF, PPI based on SVM and SAM composite were used.

References

Barton, I. F., Gabriel, M. J., Lyons-Baral, J., Barton, M. D., Duplessis, L., & Roberts, C. (2021). Extending geometallurgy to the mine scale with hyperspectral imaging: A pilot study using drone-and ground-based scanning. Mining, Metallurgy & Exploration, 38(2), 799-818.

Douglas, A., Kereszturi, G., Schaefer, L. N., & Kennedy, B. (2022). Rock alteration mapping in and around a fossil shallow intrusion at Mt. Ruapehu New Zealand with laboratory and aerial hyperspectral imaging. Journal of Volcanology and Geothermal Research, 107700. https://doi.org/10.1016/j.jvolgeores.2022.107700

Fonteneau, L. C., Martini, B., & Elsenheimer, D. (2019). Hyperspectral imaging of sedimentary iron ores–beyond borders. ASEG Extended Abstracts, 2019(1), 1-5. https://doi.org/10.1080/22020586.2019.12073201

Johnson, C. L., Browning, D. A., & Pendock, N. E. (2019). Hyperspectral imaging applications to geometallurgy: Utilizing blast hole mineralogy to predict Au-Cu recovery and throughput at the Phoenix mine, Nevada. Economic Geology, 114(8), 1481-1494. https://doi.org/10.5382/econgeo.4684

Johnson, C. L, Browning D. A., & Pendock N. E (2019). Hyperspectral imaging applications to geometallurgy: Utilizing blast hole mineralogy to predict Au-Cu recovery and throughput at the Phoenix mine, Nevada. Economic Geology, 114(8), 1481-1494.

Lorenz, S., Ghamisi, P., Kirsch, M., Jackisch, R., Rasti, B., & Gloaguen, R. (2021). Feature extraction for hyperspectral mineral domain mapping: A test of conventional and innovative methods. Remote Sensing of Environment, 252, 112129. https://doi.org/10.1016/j.rse.2020.112129

Noroozi, M., Kakaie, R., & Jalali, S. E. (2015). 3D Geometrical-Stochastical modeling of rock mass joint networks: case study of the right bank of Rudbar Lorestan Dam plant. Journal of Geology and Mining Research, 7(1), 1-10. https://doi.org/10.5897/JGMR14.0213

Qasim, M., Khan, S. D., & Haider, R. (2022). Integration of multispectral and hyperspectral remote sensing data for lithological mapping in Zhob Ophiolite, Western Pakistan. Arabian Journal of Geosciences, 15(7), 1-19. https://doi.org/10.1007/s12517-022-09788-8

Ramanaidou, E. R., & Wells, M. A. (2012). Hyperspectral imaging of iron ores. In Proceedings of the 10th International Congress for Applied Mineralogy (ICAM) (pp. 575-580). Springer, Berlin, Heidelberg.

Schodlok, M. C, Frei, M., & Segl, K. (2022). Implications of new hyperspectral satellites for raw materials exploration. Mineral Economics, 35(3), 495-502. https://doi.org/10.1007/s13563-022-00327-1

Sousa, F J, & Sousa D. J. (2022). Hyperspectral Reconnaissance: Joint Characterization of the Spectral Mixture Residual Delineates Geologic Unit Boundaries in the White Mountains, CA. Remote Sensing, 14(19), 4914. https://doi.org/10.3390/rs14194914

Stuart, M. B., Davies, M., Hobbs, M. J., Pering, T. D., McGonigle, A. J., & Willmott, J. R. (2022). High-resolution hyperspectral imaging using low-cost components: Application within environmental monitoring scenarios. Sensors, 22(12), 4652. https://doi.org/10.3390/s22124652